Scaling of ac electrical conductivity of powders under compression

M. Creyssels,* E. Falcon,† and B. Castaing
Laboratoire de Physique, Ecole normale supérieure de Lyon, CNRS, 46 allée d'Italie, 69364 Lyon Cedex 07, France
(Received 15 June 2007; revised manuscript received 16 October 2007; published 29 February 2008)

We measured, at low applied voltage, the ac electrical resistance and capacitance of a metallic powder sample under uniaxial compression. Whatever the applied stress, the frequency-dependent resistance curves can be displayed on a master curve by an appropriate rescaling. The same property is also observed for the capacitance. A one-dimensional model shows that the strong frequency dependence of the macroscopic resistance and capacitance is a consequence of the broad contact resistance distribution between grains. No microscopic model of conduction nor any parameter related to the unknown disorder need to be assumed. Relevance to other systems like random conductor-insulator mixtures or metal-cluster compounds is discussed.

DOI: 10.1103/PhysRevB.77.075135 PACS number(s): 45.70.−n, 72.80.−r

I. INTRODUCTION

For many years, many experimental, numerical, and theoretical efforts have been made to understand the ac electrical conductivity of heterogeneous materials composed of conductive and insulating constituents. The experimental results of the ac conductivity (σ) and permittivity (ϵ) in these systems are power-law dependent on the frequency ν: $\sigma \sim \nu^x$ and $\epsilon \sim \nu^{-y}$, where x is typically $0.6<x<1$, and y is found to be close to $1-x$. Such frequency response is generally named the "universal dielectric response"[1] and is observed in a wide variety of materials: metal-cluster compounds,[2,3] random conductor-insulator mixtures,[4,5] and polymer composites.[6,7] In a recent series of publications,[8–11] it has been suggested that this universal frequency-dependent conductivity and permittivity does not characterize the physical or chemical material involved, but is just an emergent property of a complex network of resistive and capacitive microstructural regions.

In this paper, we report measurements of ac conductivity of a metallic powder. This system can be electrically described by a complex network of resistors, each resistor representing one single electric contact between two grains. If the resistance values are restricted to a couple of numbers, one has a system close to a random conductor-insulator mixture. In practice, the resistances are distributed continuously between r_{min} and r_{max}, where r_{min} and r_{max} are, respectively, the minimum and the maximum of the contact resistances within the powder.

This paper is organized as follows. In Secs. II and III, we describe the experimental apparatus and give the experimental results. The complex admittance of the powder as a function of frequency follows a power-law behavior. We then describe our model and report the analytical result in Sec. IV. The powder is simply electrically modeled by a chain of resistors and capacitors in parallel. In Sec. V, a comparison with the experiments is given. Section VI is dedicated to the influence of the mechanical pressure on the frequency-dependent capacitance.

II. EXPERIMENTAL SETUP

Experiments are performed with commercial copper powder samples of 100 μm, constituted of roughly spherical particles.[12–14] The polydispersity is relatively large since the diameter of the particles varies from 50 to 110 μm.

As shown in Fig. 1, 0.5 g of powder are confined in a Plexiglass cylinder (7 mm of inner diameter), capped with two metallic electrodes (brass cylinders). The powder height is close to 2.4 mm, roughly corresponding to 500 000 particles. A mechanical pressure P rising up to 50 N/mm^2 is applied on the powder, and is measured with a static force sensor (FGP Instrumentation™, with a 0.6 mV/N sensitivity). The ac resistance and capacitance are simultaneously measured using a Hewlett Packard 4192A impedance analyzer. The amplitude of the voltage applied to the powder sample is fixed to a low value (U_{rms}=100 mV) in order to avoid any voltage-induced nonlinear effect.[14,15] The frequency ν ranges from 20 Hz to 1 MHz. Before each experimental run, the container is refilled with a new sample of powder. This procedure ensures better reproducibility than simply relaxing the confining pressure and shaking the container.

III. EXPERIMENTAL RESULTS

Figure 2 is a log-log plot of the ac resistance and ac capacitance of several copper powder samples as a function of

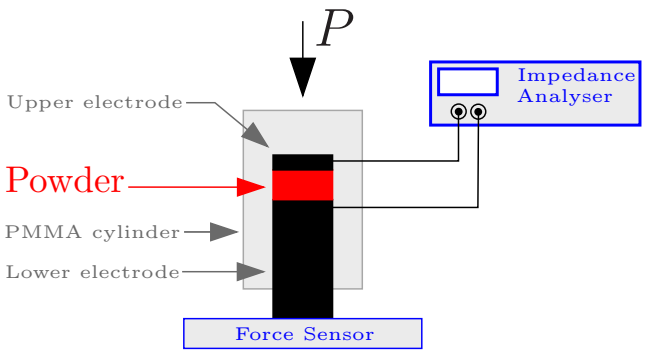

FIG. 1. (Color online) Sketch of the experimental principle. The powder sample is confined in a polymethylmethacrylate (PMMA) cylinder, capped with two metallic electrodes. A static pressure P is applied on the powder and is measured using a force sensor. An impedance analyzer is used to measure the impedance of the powder.

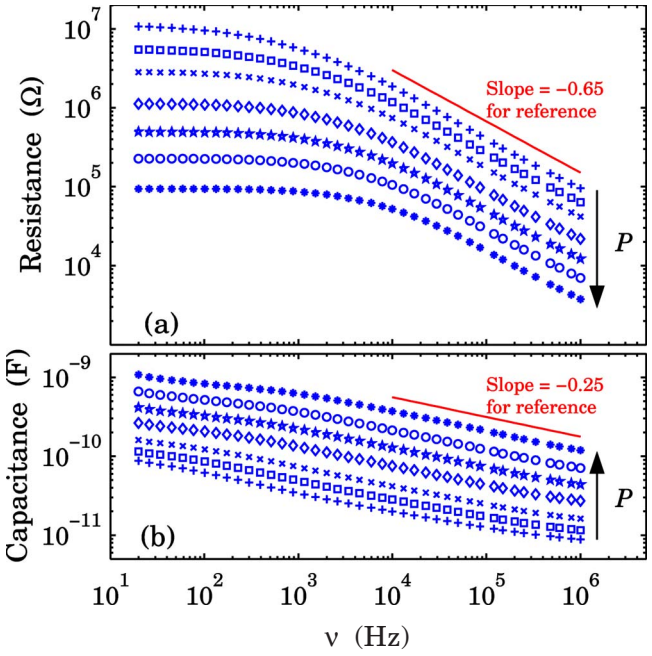

FIG. 2. (Color online) Logarithmic plot of the (a) ac resistance and (b) ac capacitance of powder samples versus frequency. Different symbols correspond to different pressures (P) applied to samples: P=4 (+), 5 (□), 8 (×), 15 (◇), 22 (⋆), 36 (○), and 52 (∗) N/mm^2. For each value of frequency, when the pressure increases, the capacitance increases, whereas the resistance decreases. At fixed pressure, both resistance and capacitance decrease with the frequency.

frequency. The pressure applied ranges from 4 to 52 N/mm^2. The complex dependence of resistance on the pressure will be studied in a future paper. At fixed pressure and low frequencies, the resistance is frequency independent. At higher frequencies, the resistance decreases and follows a power-law behavior: $R(\nu) \sim \nu^{-x}$, with x close to 0.65 [see Fig. 2(a)]. Whatever the pressure applied to the powder is, the power law is still observed and the exponent x seems to be independent of P. As for capacitance, their relative variations are smaller than those of the resistance. The capacitance is also well described by a power law: $C(\nu) \sim \nu^{-y}$, with y close to 0.25 [see Fig. 2(b)]. Finally, at high frequencies, the product RC seems to be proportional to $\nu^{-0.9}$ (Fig. 3). Besides, $RC\nu$ tends to be close to 1 when ν increases.

Such behaviors of complex admittance with frequency are observed in a very wide range of materials. To explain this ubiquity, any model must be independent of the particular physical and chemical properties of the materials involved. In our opinion, the power-law behavior does not characterize the electrical conduction at the atomic level, but it is "simply" the response of an electrical network of conventional resistive and capacitive components. Indeed, in many materials that are found to exhibit power-law behavior, we can identify resistive and capacitive microstructural regions.[8–11] That is why we simply model the powder by a network of resistors and capacitors.

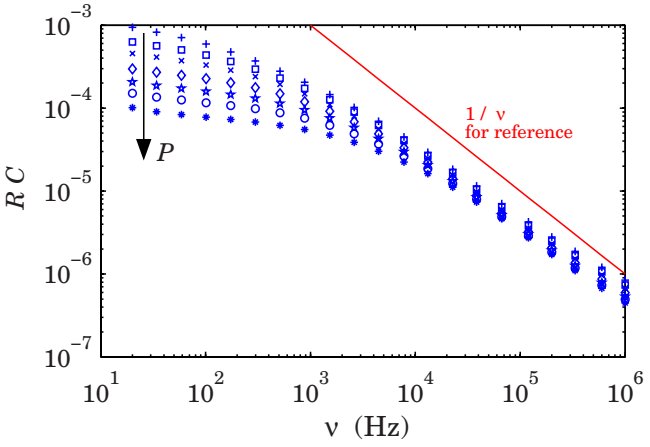

FIG. 3. (Color online) Logarithmic plot of the product RC versus frequency. Same symbols as in Fig. 2.

IV. MODEL AND ITS ANALYTICAL RESULTS

The powder is a set of conductive copper grains in contact. Its high electrical resistance is probably due to an oxide layer on the grain surface. As a consequence, the contact between two metallic grains can be electrically described by a resistor (r) and a capacitor (c) in parallel. A suitable representation of the whole powder is then a three-dimensional network of connected $r\|c$ circuits, where r is the resistance and c the capacitance of each grain-grain contact. However, to simplify our model, only one conductive path is assumed to connect the lower to the upper electrode [see Fig. 4(a)]. We will then show that this one-dimensional model is really sufficient to describe correctly the frequency behavior of both resistance and capacitance observed in Fig. 2. Besides, the number N of grain-grain contacts is choosen large enough to allow a statistical evaluation of the impedance of this system.

To complete the model, we have to know the form of the distribution functions of the contact resistances $\mathcal{P}(r)$ and of the contact capacitances $\mathcal{Q}(c)$. Intuitively, these two distributions depend on the physical and chemical properties of the oxide on the grain surface. Here, we suggest that the strong frequency dependence of the equivalent resistance R and the equivalent capacitance C [see Fig. 4(b)] is directly caused by the distributions $\mathcal{P}(r)$ or $\mathcal{Q}(c)$ being broad enough.

First, the assumption that $\mathcal{P}(r)$ is broad seems quite reasonable and consistent with some experimental observations.

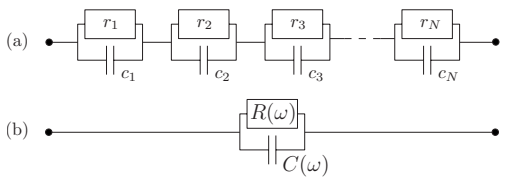

FIG. 4. (a) The electrical properties of the powder are simply modeled by a chain of N $r\|c$ circuits. (b) Electrical equivalent circuit of the chain. The equivalent resistance R and the equivalent capacitance C depend on the frequency ν or on the angular frequency $\omega=2\pi\nu$.

Indeed, in recent works,[15,16] we showed that the contact resistances between stainless steel beads are widely distributed, probably as a consequence of the inhomogeneity of the oxide layer. The distribution of resistance was well fitted by a lognormal distribution.

Second, in the Appendix, we demonstrate that the distribution function of the product $\tau=rc$ must be broad enough to reproduce well the measured equivalent impedance of the powder. We note $\tau_{\max}$ and $\tau_{\min}$ the largest and the smallest characteristic times, respectively, of the N $r\|c$ circuits. At very low frequencies [i.e., $\nu(r)\ll 1/\tau_{\max}$] and also at very high frequencies (i.e., $\nu\gg 1/\tau_{\min}$), the total resistance of a chain of $r\|c$ circuits is frequency independent. The ratio between the resistance when the frequency is low (R_0) and its value when the frequency is high (R_{hf}) is lowest than the ratio between $\tau_{\max}$ and $\tau_{\min}$: $R_0/R_{hf}<\tau_{\max}/\tau_{\min}$. The experimental data indicate that R_0/R_{hf} is greater than 100 (Fig. 2). So, in our model, we must take $\tau_{\max}/\tau_{\min}>100$.

We now make some assumptions on the form of $\mathcal{P}(r)$ and $\mathcal{Q}(c)$ which are very useful from an analytical point of view. For $\mathcal{P}(r)$, we do not use a lognormal distribution (as in Refs. 15 and 16), but use a simple flat distribution of resistance logarithms. We suppose that the contact resistances between copper grains (r) are such that the probability density of their logarithm is uniform with the value $\mathcal{P}_0$ for $\ln r_{\min}<\ln r<\ln r_{\max}$. As for the capacitances, the distribution $\mathcal{Q}(c)$ is chosen as simple as possible since we suppose that all capacities c are equal to a constant value c_0. Thus, the distribution of the characteristic time $\tau=rc$ is broad because it is also $\mathcal{P}$. Beyond simplicity, $\mathcal{Q}$ is choosen very different from $\mathcal{P}$ since, until now, no experiment has shown that the contact capacitances are widely distributed, contrary to the contact resistances.

Finally, our model depends on three parameters: c_0, $r_{\max}$, and $\eta=r_{\min}/r_{\max}\ll 1$:

$$c=c_0, \tag{1}$$

$$\mathcal{P}(r)=\mathcal{P}_0/r, \tag{2}$$

where $\mathcal{P}_0=-1/\ln\eta$, due to normalization.

The total impedance predicted by the above model is NZ with

$$Z=\int_{r_{\min}}^{r_{\max}}\frac{r}{1+jrc_0\omega}\mathcal{P}(r)dr=\frac{z_1-jz_2}{c_0\omega}, \tag{3}$$

where

$$z_1=\int_{r_{\min}}^{r_{\max}}\frac{rc_0\omega}{1+r^2c_0^2\omega^2}\mathcal{P}(r)dr, \tag{4}$$

$$z_2=\int_{r_{\min}}^{r_{\max}}\frac{r^2c_0^2\omega^2}{1+r^2c_0^2\omega^2}\mathcal{P}(r)dr. \tag{5}$$

The powder can be described electrically by a resistor and a capacitor in parallel, both are frequency dependent:

$$\frac{1}{NZ}=\frac{1}{R(\omega)}+jC(\omega)\omega \tag{6a}$$

$$=\frac{z_1}{z_1^2+z_2^2}\frac{c_0\omega}{N}+j\frac{z_2}{z_1^2+z_2^2}\frac{c_0\omega}{N}. \tag{6b}$$

From Eqs. (6a) and (6b), the evolution of $RC\omega$ as a function of the angular frequency ω then is

$$RC\omega=\frac{z_2}{z_1}. \tag{7}$$

In the case of a flat distribution of resistance logarithms [Eq. (2)], explicit integration of z_1 and z_2 is possible, and Eq. (7) becomes

$$RC\omega=\frac{1}{2}\frac{\ln(1+r_{\max}^2c_0^2\omega^2)-\ln(1+r_{\min}^2c_0^2\omega^2)}{\arctan(r_{\max}c_0\omega)-\arctan(r_{\min}c_0\omega)}. \tag{8}$$

At low enough frequency, the product RC is very close to a constant R_0C_0:

$$R_0C_0=\frac{1+\eta}{2}r_{\max}c_0\simeq\frac{r_{\max}c_0}{2}. \tag{9}$$

Measuring RC at very low frequency, thus, gives the value of the product $r_{\max}c_0$. It follows that

$$\frac{RC}{R_0C_0}=\frac{1}{\Omega}\frac{\ln(1+\Omega^2)-\ln(1+\eta^2\Omega^2)}{\arctan(\Omega)-\arctan(\eta\Omega)}, \tag{10}$$

where $\Omega=2R_0C_0\omega$ is the adimensional angular frequency. Since η is close to zero, a good approximation is to neglect terms containing η in Eq. (10). These theoretical results show that RC/R_0C_0 is a "universal" function of Ω since it has no adjustable parameter and is independent of the pressure and the physical properties of the oxide. Finally, the dependence of resistance and capacitance on Ω can be expressed for $\eta=0$:

$$\frac{R}{R_0}=\frac{1}{\Omega}\frac{[\arctan(\Omega)]^2+\frac{1}{4}[\ln(1+\Omega^2)]^2}{\arctan(\Omega)}, \tag{11}$$

$$\frac{C}{C_0}=\frac{\ln(1+\Omega^2)}{[\arctan(\Omega)]^2+\frac{1}{4}[\ln(1+\Omega^2)]^2}. \tag{12}$$

V. COMPARISON WITH THE EXPERIMENTS

Figure 5 is a log-log plot of RC/R_0C_0 as a function of adimensionnal angular frequency Ω, comparing both the model of Sec. IV and the experimental data of Sec. III. R_0 and C_0 are simply the measured values of the resistance and the capacitance at 20 Hz, respectively.

The rescaling predicted in our model [Eq. (10)] is almost perfect. Moreover, in order to have good agreement with the data, η has to be smaller than 10^{-5} (see Fig. 5). This means that the distribution of resistances is broad: $r_{\min}<10^{-5}r_{\max}$. However, the model slightly overestimates RC/R_0C_0.

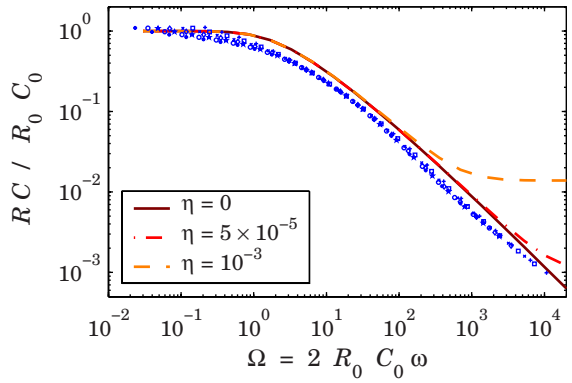

FIG. 5. (Color online) Logarithmic plot of RC/R_0C_0 versus Ω, for different pressures applied to the powder. The lines correspond to Eq. (10) with η going from 0 to 10^{-3}.

Figures 6(a) and 6(b) display the variations of R/R_0 and C/C_0 as a function of Ω. For comparison, the predictions from Eqs. (11) and (12) are also shown. Two observations can be made. First, using the adimensional angular frequency Ω and rescaling the resistance by its value at low frequency, all curves R *vs* ω fall on the same master curve whatever the pressure applied to the powder. Second, our model provides a correct scaling function R/R_0 *vs* Ω without using any adjustable parameter.

The rescaling is also acceptable for the capacity [Fig. 6(b)] and the model reproduces well the general trend. Differences between rescaled experimental data and model predictions are greater for the capacity than for the resistance. It is certainly due to the simplicity of our model, in particular, all grain-grain contacts are supposed to have the same capacity c_0.

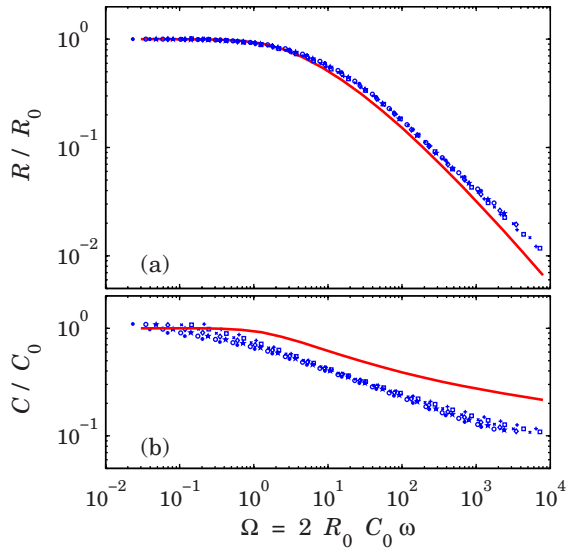

FIG. 6. (Color online) (a) Rescaled resistance as a function of rescaled angular frequency for various pressures applied to the powder. The solid line is the prediction from Eq. (11). (b) Rescaled capacitance as a function of Ω. The solid line shows the behavior predicted by our model [Eq. (12)].

VI. CAPACITANCE VERSUS MECHANICAL PRESSURE AND FREQUENCY

In other experimental works[14,17] dedicated to the influence of mechanical pressure on the DC electrical properties of a powder sample, we show that both resistance and capacitance follow a power-law behavior like

$$R_0(P) \sim P^{-\alpha_0}, \tag{13}$$

$$C_0(P) \sim P^{\beta_0}, \tag{14}$$

where $\alpha_0 \approx 1.7$ and $\beta_0 \approx 1$. R_0 and C_0 are the resistance and the capacitance at low frequencies.

In this section, we investigate the influence of frequency on the power-law dependence of capacitance with the mechanical pressure. For any fixed frequency ν arbitrarily chosen between 20 Hz and 1 MHz, the capacitance as a function of pressure can be approximately fitted by a power law in the pressure range from 4 to 50 N (see Fig. 7):

$$C(\omega, P) \sim P^{\beta_\omega}. \tag{15}$$

The exponent β_ω remains close to 1, but depends slightly on the angular frequency $\omega = 2\pi\nu$ (see Fig. 8).

Interpretation

Equation (12) describes the evolution of the capacitance with both angular frequency and pressure. It can be rewritten in a more appropriate form as

$$C(\omega, P) = C_0(P)\mathcal{F}(\Omega). \tag{16}$$

As $\Omega = 2R_0C_0\omega$, with R_0 and C_0 pressure dependent, $\mathcal{F}(\Omega)$ varies with P at fixed ω. We show below that we can fit this variation with a power law in pressure in the limited explored range $P_{\min} < P < P_{\max}$, with $P_{\min} = 4$ and $P_{\max} = 50\ \mathrm{N/mm^2}$ [see Fig. 7 and Eq. (15)]. We define $P_m = \sqrt{P_{\min}P_{\max}}$ such that $\ln \Omega(\omega, P_m)$ is the center of the variation interval of $\ln \Omega(\omega, P)$ at fixed ω [see Eqs. (13) and (14)]:

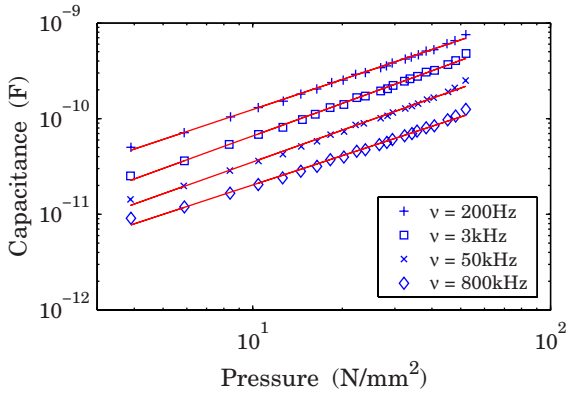

FIG. 7. (Color online) The capacitance as a function of mechanical pressure for four particular frequencies: 200 Hz (+), 3 kHz (□), 50 kHz (×), and 800 kHz (◇). Solid lines are power-law fits $C \sim P^{\beta_\omega}$, with $0.98 < \beta_\omega < 1.14$. At low and high pressures, there are small curvatures of the data.

$$\Omega(\omega,P)=\Omega(\omega,P_m)\left(\frac{P}{P_m}\right)^{\beta_0-\alpha_0}. \quad (17)$$

In this limited range of Ω, we can approximate $\mathcal{F}(\Omega)$ as

$$\mathcal{F}(\Omega)\sim\Omega^{-\Upsilon(\omega)}, \quad (18)$$

where

$$\Upsilon(\omega)=-\frac{d\ln\mathcal{F}}{d\ln\Omega}[\Omega=\Omega(\omega,P_m)]. \quad (19)$$

Finally, according to our model described in Sec. IV, the capacitance remains a power law of pressure for any angular frequency:

$$C(\omega,P)=C(\omega,P_m)\left(\frac{P}{P_m}\right)^{\beta_\omega}, \quad (20)$$

with

$$\beta_\omega=\beta_0+(\alpha_0-\beta_0)\Upsilon(\omega). \quad (21)$$

We report in Fig. 8 the exponent β_ω [defined by Eq. (15)] as a function of the frequency. The experimental results exhibit good agreement with the theoretical prediction [Eq. (21)] obtained with our simple electrical model of powder. We stress here that there is no fitted or adjustable parameter in this approach. Besides, Eq. (21) shows that β_ω depends not only on the angular frequency, but also on the arbitrary pressure P_m (see also Fig. 8). Since β_ω is not strictly pressure independent, according to our model, the power-law behavior of capacitance as a function of the pressure [Eq. (15)] cannot be valid when the pressure is largely lower or largely higher than P_m. Experimentally, such deviations from this power law are seen at low and high pressures (Fig. 7), and they might be explained by the variations of the exponent β_ω predicted by our model.

Similarly, one can extend this analysis to the resistance behavior as a function of the pressure and the frequency. However, at fixed pressure, the capacitance is close to a power law of Ω [Fig. 6(b)], whereas the resistance cannot be considered as a power law of Ω [Fig. 6(a)]. The approximation (18) is then not valid for the resistance. So, the relative variations of the resistance with pressure and frequency are much more complex to interpret than those of the capacitance.

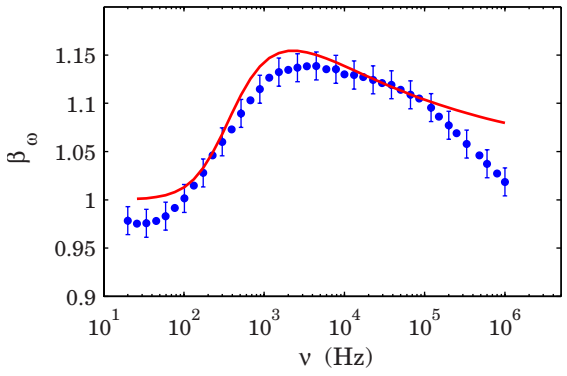

FIG. 8. (Color online) Frequency dependence of the power-law exponent β_ω. (●) experiments from the power-law fits of Fig. 7. At low and high frequencies, $\beta_\omega\approx\beta_0=1$. The solid line shows the behavior expected from our model with $P_m=15$ N [Eq. (21)]. According to Eq. (21), β_ω depends slightly on the pressure P_m, so β_ω varies a little bit with the range of pressure chosen in Fig. 7.

VII. CONCLUSION AND RELEVANCE TO OTHER PHYSICAL SYSTEMS

This work has shown that the electrical characteristics of a metallic powder are simply those of an electrical network formed by a large number of pure resitors and pure capacitors in random position. At high enough frequencies, the observed power-law dependence on the frequency of the ac resistance and capacitance originates from a broad resistance variability of the contact between grains. ac measurements have given precious hints on the distribution of resistances and capacitances that are compatible with a wide distribution of resistances and a narrow distribution of capacitances.

For such a granular medium, we have demonstrated that a simple one-dimensional model can easily describe the frequency-dependent impedance observed. For this, no microscopic model of conduction nor any parameters related to the unknown disorder need to be assumed. Similar behavior of the complex impedance has been observed in many heterogeneous materials (random conductor-insulator mixtures, metal-cluster compounds, etc.). We suggest that our interpretation remains valid in other materials containing a large variability of resistance and capacitance phases.

APPENDIX: ELECTRICAL BEHAVIOR OF A CHAIN OF $r\|c$ CIRCUITS AT LOW AND HIGH FREQUENCIES

Let us consider the low- and high-frequency limits of the equivalent resistance $R(\omega)$ and the equivalent capacitance $C(\omega)$ in the model described in Fig. 4. Here, no assumption is made on the distribution of resistance $\mathcal{P}(r)$ or on the distribution of capacitance $\mathcal{Q}(c)$. The total impedance of the chain is the sum of the individual impedances of the $r\|c$ circuits and it can also be described by a resistance $R(\omega)$ in parallel with a capacitance $C(\omega)$ depending both in the angular frequency ω:

$$Z=\sum_{i=1}^{N}\frac{r_i}{1+j\tau_i\omega}=\frac{R}{1+jR(\omega)C(\omega)\omega}, \quad (A1)$$

with $j^2=-1$.

At very low frequencies ($\omega\ll 1/\tau_{\max}$), the impedance of each capacitor c_i is broadly smaller than its corresponding resistance r_i. Then, Z can be approximated by

$$Z\approx\sum_{i=1}^{N}r_i-j\sum_{i=1}^{N}\tau_i r_i\omega=R-jR^2C\omega. \quad (A2)$$

So, when $\omega\ll 1/\tau_{\max}$, the resistance and the capacitance are found to be independent of ω and are equal to

$$R_0=\sum_{i=1}^{N}r_i=\sum_{i=1}^{N}\tau_i/c_i, \quad (A3)$$

$$C_0 = \frac{\sum_{i=1}^{N} r_i \tau_i}{\left(\sum_{i=1}^{N} r_i\right)^2}. \tag{A4}$$

On the contrary, at very high frequencies ($\omega \gg 1/\tau_{\min}$), every resistance r_i is broadly smaller than the impedance of its corresponding capacitor c_i. Equation (A1) becomes

$$Z \approx \sum_{i=1}^{N} \frac{r_i}{j\tau_i\omega} + \sum_{i=1}^{N} \frac{r_i}{\tau_i^2\omega^2} = \frac{1}{jC\omega} + \frac{R}{R^2C^2\omega}. \tag{A5}$$

When the frequency is sufficiently high, R and C are frequency independent:

$$R_{hf} = \frac{\left(\sum_{i=1}^{N} r_i/\tau_i\right)^2}{\sum_{i=1}^{N} r_i/\tau_i^2} = \frac{\left(\sum_{i=1}^{N} 1/c_i\right)^2}{\sum_{i=1}^{N} 1/(c_i\tau_i)}, \tag{A6}$$

$$C_{hf} = \frac{1}{\sum_{i=1}^{N} r_i/\tau_i}. \tag{A7}$$

We deduce from Eqs. (A3) and (A6) that the ratio R_0/R_{hf} can be written as

$$R_0/R_{hf} = \langle \tau_i \rangle_{\{c_i\}} \times \langle 1/\tau_i \rangle_{\{c_i\}}, \tag{A8}$$

where $\langle x_i \rangle_{\{y_i\}}$ is the weighted average of data $\{x_i\}$ with corresponding weights $\{y_i\}$.

Similarly, from Eqs. (A4) and (A7), the ratio C_0/C_{hf} can be written as the product of the weighted average time $\langle \tau_i \rangle_{\{r_i\}}$ by the weighted average of inverse time $\langle 1/\tau_i \rangle_{\{r_i\}}$:

$$C_0/C_{hf} = \langle \tau_i \rangle_{\{r_i\}} \times \langle 1/\tau_i \rangle_{\{r_i\}}. \tag{A9}$$

Finally, Eqs. (A8) and (A9) show that ratios R_0/R_{hf} and C_0/C_{hf} are smaller than the ratio $\tau_{\max}/\tau_{\min}$.

*mathieu.creyssels@ens-lyon.fr
†Present address: Matière et Systèmes Complexes, Universitè Paris-Diderot, Paris 7, CNRS, 75 013 Paris, France.

[1] A. K. Jonscher, Nature (London) **267**, 673 (1977).
[2] J. A. Reedijk, L. J. Adriaanse, H. B. Brom, L. J. de Jongh, and G. Schmid, Phys. Rev. B **57**, R15116 (1998).
[3] A. M. Farid, H. E. Atyia, and N. A. Hegab, Vacuum **80**, 284 (2005).
[4] Yi Song, Tae Won Noh, Sung-Ik Lee, and James R. Gaines, Phys. Rev. B **33**, 904 (1986).
[5] R. K. Chakrabarty, K. K. Bardhan, and A. Basu, J. Phys.: Condens. Matter **5**, 2377 (1993).
[6] D. S. McLachlan and M. B. Heaney, Phys. Rev. B **60**, 12746 (1999).
[7] K.-M. Jäger, D. H. McQueen, I. A. Tchmutin, N. G. Ryvkina, and M. Klüppel, J. Phys. D **34**, 2699 (2001).
[8] D. P. Almond and B. Vainas, J. Phys.: Condens. Matter **11**, 9081 (1999).
[9] R. Bouamrane and D. P. Almond, J. Phys.: Condens. Matter **15**, 4089 (2003).
[10] D. P. Almond and C. R. Bowen, Phys. Rev. Lett. **92**, 157601 (2004).
[11] K. D. Murphy, G. W. Hunt, and D. P. Almond, Philos. Mag. **86**, 3325 (2006).
[12] Goodfellow product catalogue No. CU 006025, 2004; see also http://www.goodfellow.com/
[13] E. Falcon, B. Castaing, and C. Laroche, Europhys. Lett. **65**, 186 (2003).
[14] M. Creyssels, Ph.D. thesis, Laboratoire de Physique, Ecole Normale Supérieure de Lyon, 2007.
[15] M. Creyssels, S. Dorbolo, A. Merlen, C. Laroche, B. Castaing, and E. Falcon, Eur. Phys. J. E **23**, 255 (2007).
[16] S. Dorbolo, A. Merlen, M. Creyssels, N. Vandewalle, B. Castaing, and E. Falcon, Europhys. Lett. **79**, 54001 (2007).
[17] M. Creyssels, E. Falcon, and B. Castaing (unpublished).